MEASUREMENT AND CORRELATION OF CLEAR LIQUID HEIGHT ON SMALL HOLE DISTILLATION SIEVE TRAY

L. T. Fan[1], X.G. Yuan[1]*, A. W. Zeng[1], K.T. Yu[1], M. Kalbassi[2] and K. E. Porter[3]

[1] State Key Laboratory of Chemical Engineering, Tianjin 300072, China, Email: yuanxg@tju.edu.cn
[2] Air Products PLC. UK
[3] Aston University, UK

Abstract
The present paper reports an experimental study in measuring the clear liquid height and its gradient along the flowing path direction of the liquid on an experimental tray with small sieve holes and of industrial-scale. The experiments were performed with water and air in a rectangular tray installed within a column of 1.2m inner diameter. The experimental results under various operating conditions are compared with a number of published empirical and semi-theoretical correlations. The models are recorrelated and suitable correlations for predicting the clear liquid height on small-hole sieve trays are recommended.

Keywords: Fluid dynamic behaviour, clear liquid height, small-hole sieve tray

1. Introduction

The performance of distillation trays is greatly affected by the clear liquid height, because it gives influence not only on the liquid bed pressure drop, but also on the residence time of the vapor-liquid two-phase flow in trays, the interfacial area and then on the separation efficiency. So an adequate estimation of the clear liquid height of tray is of importance for proper design of distillation columns. A number of reliable correlations for clear liquid height estimating are available in the literatures [1-6, 8].

Previous works on the clear liquid height were more concentrated in the normal size hole, and reliable clear liquid height data for small hole tray have been rarely reported. Small-hole sieve trays are widely used in clean services such as air separation columns. Small sieve holes may enhance the tray capacity in terms of entrainment limit and tend to generate emulsion regime of the two-phase flow on trays. In this work the hydraulic gradient for small hole sieve tray is experimentally investigated and some available models for clear liquid height are recorrelated and compared. The experiments were conducted with air and water in an industrial scale column in which a test tray with a rectangular active (bubbling) area was installed.

2. Experiment

2.1 Experimental Installation

The schematic diagram of experimental installation is shown in figure 1a and the geometric parameters are given in table 1. The air is introduced in the bottom of the column. A gas distributing tray is installed below the test tray to generate an even gas flow distribution similar to real world operation. The air flowrate was regulated by means of a two rotary vanes at the blower inlet and outlet respectively and measured by means of a D-type tube and calibrated by a Pitot tube. Water is pumped into the top of the column, and a short section of random packing (25 mm Raschig rings) bed is used to spread the fed liquid in the inlet downcomer of the test tray. The flow rate of water was measured by a rotameter for lower rates and by a vortex flowmeter for higher ones. The water flowrate was controlled by a stop valve. The clearance under the downcomer is 33 mm and the tray spacing is 450 mm.

The geometrical details of the test tray are shown in figure 1c and the related parameters are given in Table 1. As shown in figure 1b and c, nine U-tubes, like those of hydrostatic gauges that are usually used in the tray hydraulic measurements,[5] were used to measure the clear liquid height on the small hole sieve tray. As probes, the mouths of one end of the U-tubes were arranged on the central line of the test tray along the flow path direction. As shown in the figures, fine mashes screening the probe mouths from disturbance of the two-phase fluid turbulences on the tray, and capillary tubes inserted into the U-tubes are used to stabilize the measurement readings.

a. Experimental installation

b. U-tube measuring system for clear liquid height

c. Geometric structure of test tray
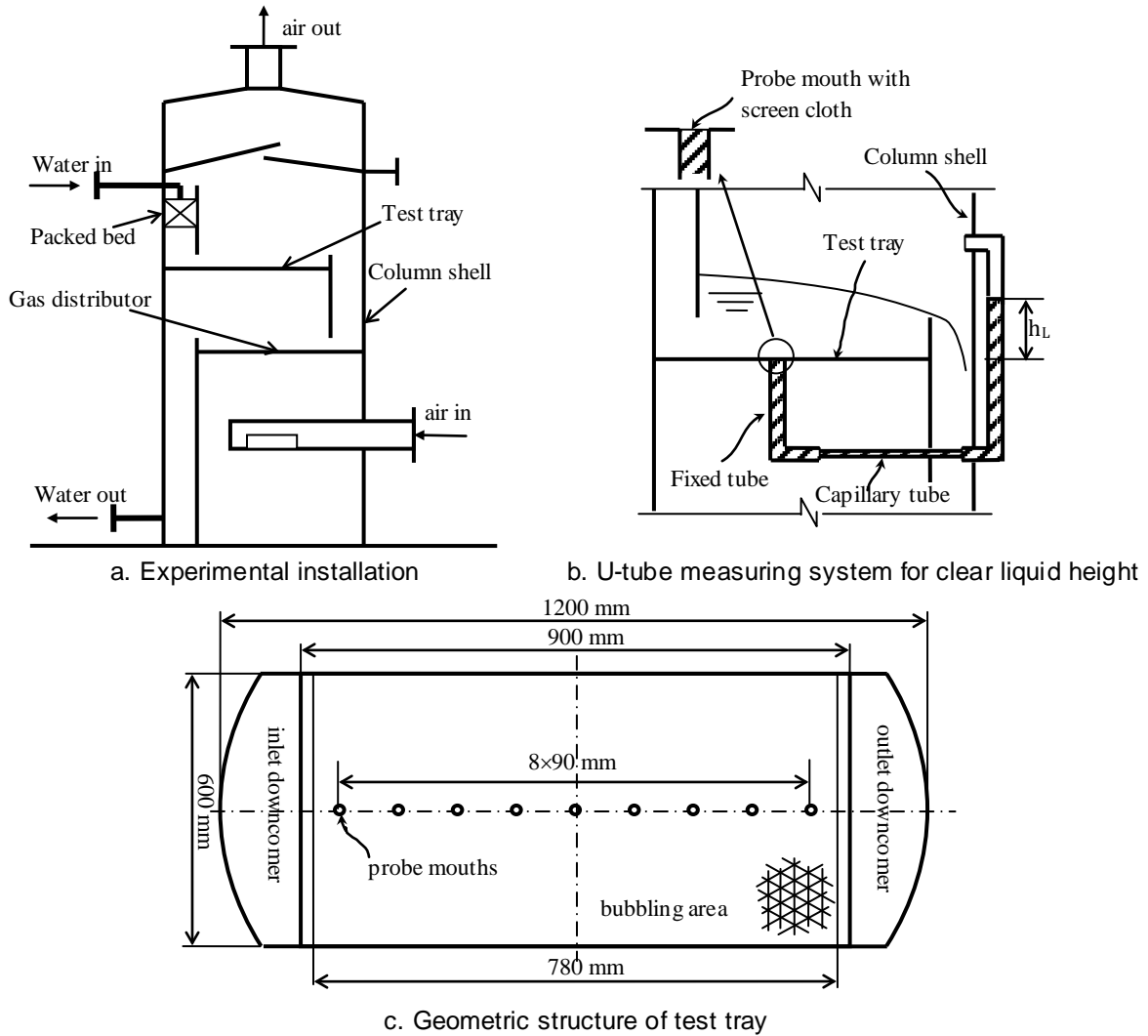
Figure 1. Schematic diagram and structure of experimental installation

Table 1. Parameters for the experimental installation

Parameter	Unit	Value
Column diameter (D)	mm	1200
Tray spacing (H)	mm	450
Tray path length (l_t)	mm	900
Weir length (l_w)	mm	680
Bubbling area (A_b)	mm^2	780×600
Tray thickness (δ)	mm	1
Length of inlet calming section (l_i)	mm	60
Length of outlet calming section (l_o)	mm	60
Diameter of sieve holes (d)	mm	1
Hole spacing (p)	mm	3.2
Holes pitch	-	Equilateral triangular
Open area of total bubbling area (ε)	%	8.856

2.2 Measurements and Results

Three readings were averaged to give a local clear liquid height for an operating condition in the experiments. Some of the measurement results on the clear liquid heights are plotted in Figure 2, and the data for zero weir height are listed in Appendix, The figures show the variations of clear liquid

height (h_C) with the distance (x) in the flowing path for different values of gas hole kinetic factor (F) , liquid flow rate per outlet weir length (L_w) and outlet weir height. The abscissa (x) is the distance from liquid inlet to measurement point. It can be seen from these figures that in general, the clear liquid height increases with the increase of liquid flow rate and that of the height of outlet weir, and decreases with the increase of gas hole kinetic factor. This behaviors are found to be consistent with those for the normal hole sized trays[1]. Figure 2 also demonstrates that hydraulic gradients exist on the small-hole tray. Generally, clear liquid height decreases from inlet (x=9 cm) to outlet (x=81 cm), and the fall (the gradient) decreases with the decrease of liquid flow rate and the increase of outlet weir height. As noted in fig.2, for the low weir liquid flow rate, higher hole f-factor increases the hydraulic gradient, just as long being observed, however, for the high liquid flow rate, increasing the f-factor may reduce the hydraulic gradient. For lower f-factor, a large clear liquid height can be seen near the inlet, followed by a sharp decline. This phenomenon due to the absence of inlet weir has also observed previously [5]. In general, the increase of gas hole kinetic factor may increase the liquid flow resistance, and at the same time, aerate the liquid to give a froth operation regime. In the case of small hole tray with higher liquid load and f-factor, the second effect of the high f-factor might become dominant. This may explain the phenomena observed in our experiments.

3. Models for clear liquid height

3.1 Experimental Results Analysis

The clear liquid heights of the nine locations are averaged to give the average clear liquid height of the tray in this work. Figure 3 gives the plots of the averaged clear liquid height varying with different influential factors, which are usually employed for modeling purpose. These are: gas hole kinetic factor F, liquid flowrate per unit length of outlet weir L_w and the height of the outlet weir h_w.

a. Without outlet weir

b. Height of outlet weir=20 mm

c. Height of outlet weir= 35 mm

d. Height of outlet weir= 50 mm
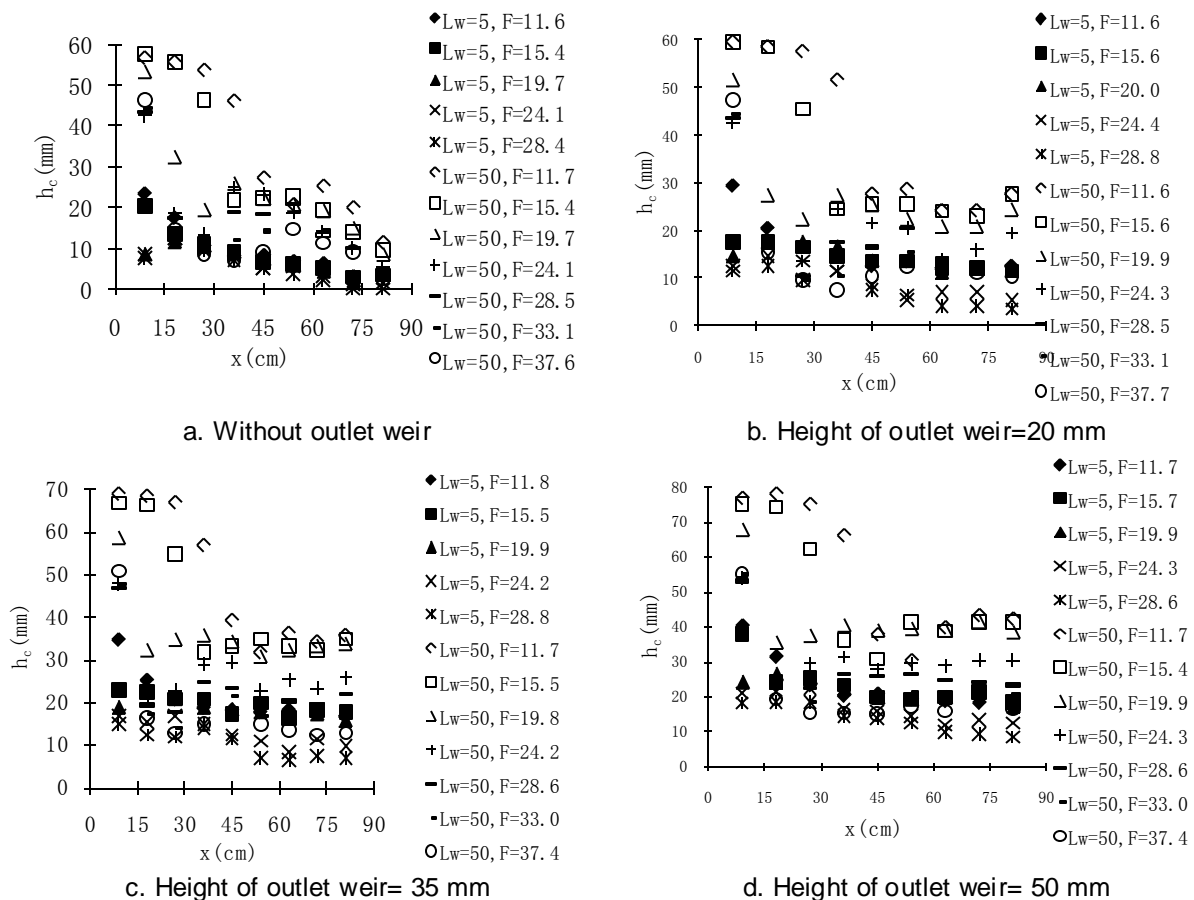
Figure 2. Clear liquid height distributions of the small hole tray
F: hole f-factor (m/s).(kg/m^3)$^{0.5}$; Lw: liquid flowrate m^3/(h.m of length of outlet weir)

a. Effect of gas hole kinetic factor   b. Effect of liquid load per unit outlet weir length

c. Effect of height of outlet weir
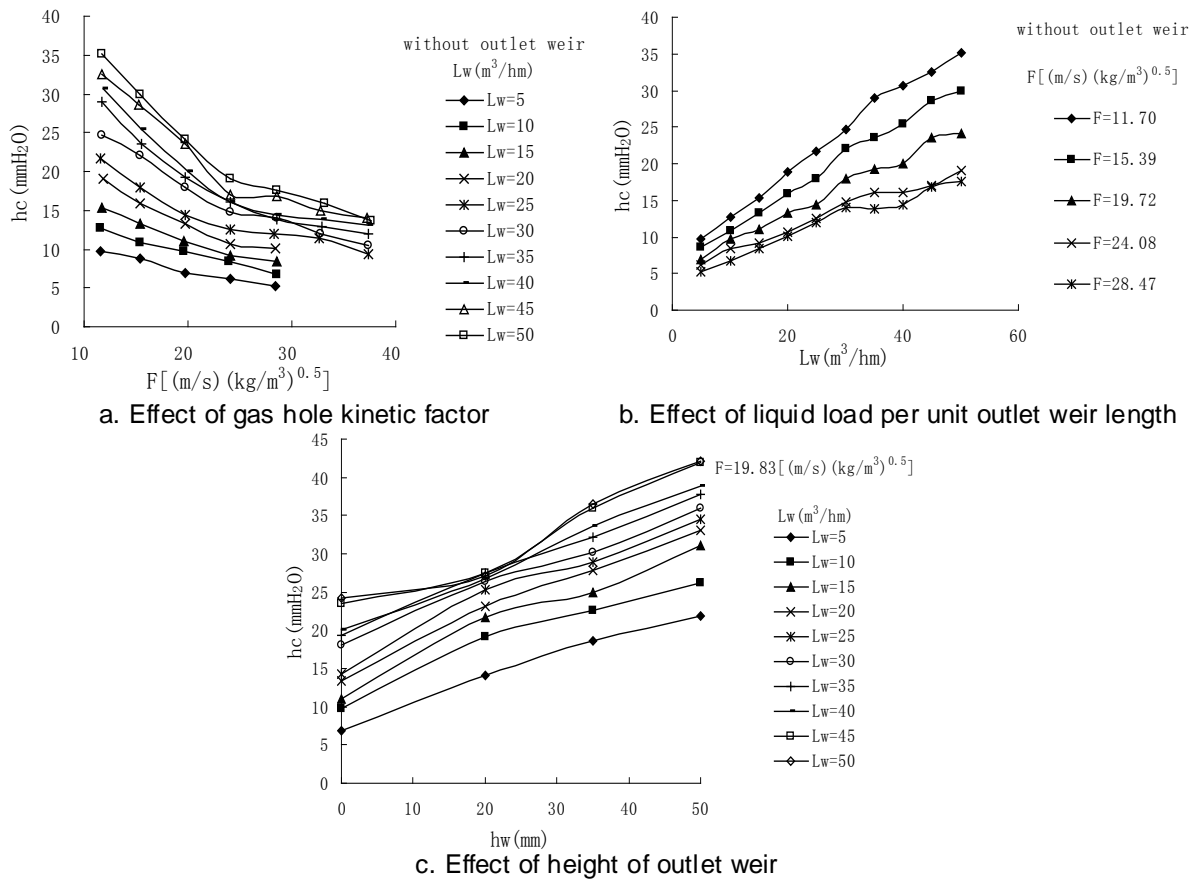
Figure 3. Variations of average clear liquid height

Overall, it can be seen from figure 3 that the increases in the liquid flow rate and the height of the outlet weir, and decreasing the gas hole kinetic factor may favor the accumulation of liquid on the tray. The plots in figure 3 demonstrate also that the clear liquid heights vary linearly with the influential factors except for some of those with the gas hole kinetic factor.

3.2 Available Models and Evaluations

Two approaches to modeling the clear liquid height of distillation tray can be found in the literatures: semi-theoretical based models and experimental correlations. The model developed by Colwell et al.[2] and then simplified and improved by Bennett et al.[3] can be known as the representatives for the first category. These models are based on the weir equation proposed by Fancis [7]. The model of Bennett et al. can be written as

$$h_C = \phi_e \left[h_W + C \left(\frac{L_W}{\phi_e} \right)^{2/3} \right]$$ (1)

where the froth density ϕ_e and the weir coefficient C are given respectively by

$$\phi_e = \exp\left(-C_A K_s^{C_B}\right) \quad \text{and} \quad C = C_C - C_D \exp\left(-C_E h_W\right)$$ (2)

The gas flow parameter K_s is written as $K_s = V_s \left(\dfrac{\rho_V}{\rho_L - \rho_V} \right)^{1/2}$, V_s is the a superficial velocity of gas on the

active area basis in m/s. Coefficients C_A through C_E are experimentally determined constants. It can be seen from equation (1) and (2) that the model interprets the influences of the outlet weir height, liquid load per unit weir length and the gas kinetic energy. Another widely used model, developed by Jacimovic et al.[8], is written as

$$h_C = (C_F + C_G h_W)\sqrt{F_{\lg}} \tag{3}$$

where the flow parameter $F_{\lg}$ represents a ratio of liquid to gas kinetic energy: $F_{\lg} = \dfrac{V_L}{V_G}\sqrt{\dfrac{\rho_G}{\rho_L}}$, and C_F and C_G are again the constants to be determined experimentally. A model of the second category, empirical correlation to experimental data, can be as simple as that given by Huang and Wang.[9]

$$h_C = C_0 + C_1 h_W^{0.5} + C_2 L_W + C_3 F^2 + C_4 F \tag{4}$$

where F is the hole gas f-factor and C_0 through C_4 are constants to be determined by data fitting. The application of such a model may be subject to limitations from the experimental conditions.

The correlations represented by equation (1), (3) and (4) are applied to estimate the clear liquid height for the experimental tray in this work. The comparison of the predicted and experimental results is shown in figure 4a. The models are also evaluated in terms of *standard deviation* Δ and *correlation ratio* Θ (a good correlation is featured by a small Δ and a value of Θ approaching to 1), and the results are given in Table 2. It can be seen from the table that the Jacimovic model gives better predictions than the two others.
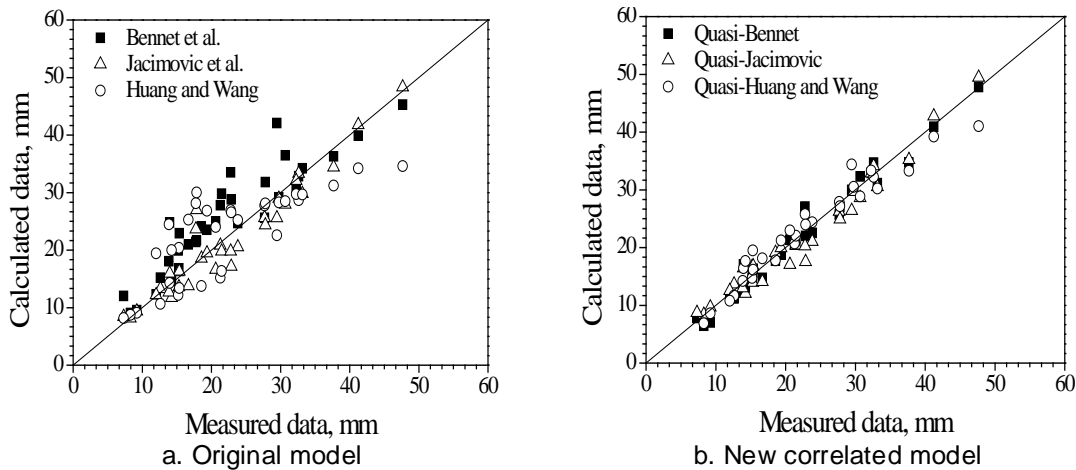
Figure 4. Parity plot of measured vs predicted clear liquid height for the small sieve tray

Table 2. Evaluation of correlations

Reference	Original correlation		New correlated model		New correlated constants***
	Δ, %*	Θ**	Δ, %*	Θ**	
Bennet et al.[3]	28.24	0.8493	9.81	0.9853	C_A=,16.66 C_B=0.82, C_C=1.0648, C_D=0.264, C_E=37.23
Jacimovic et al.[8]	14.74	0.9531	15.04	0.9551	C_F=41, C_G=0.92,
Huang and Wang[9]	64.16	-	20.06	0.9623	C_0=7.6, C_1=2.439, C_2=220, C_3=1.74×10⁻², C_4=1.699×10⁻²

* $\Delta = \sqrt{\sum_1^n [(z_i - z_i^C)/z_i]^2 / n}$, ** $\Theta = \sqrt{1 - \sum_1^n (z_i - z_i^C)^2 / \sum_1^n (z_i - z_{av})^2}$

z=experimental date, z_{av}=average of z, z^C=predicted value, n=number of experimental data

*** the unit system: h_W(m), h_C(m), L_W(m³/min.cm) was applied in the correlation

3.3 Re-correlations of the Models

In this subsection, models of equation (1), (3) and (4) are used to fit the experimental data reported in section 3.1 and the least square method is used to solve for the constants in the equations. As a result, the constants obtained for the new correlations are given in the last column of table 2 and the comparison of the predicted and experimentally measured clear liquid height data is shown in figure 4b. Then, the new correlated models are evaluated with the *standard deviation* and the *correlation ratio,* and the results are shown in table 2. It can be seen from table 2 and figure 4b that the new correlated constants strengthen the correlations for all the three models. The best predictions are given by the model of Bennett et al.[3] with the new correlated constant. Comparing the evaluations of the original with the new correlated models, the model of Bennett et al.[3] and that of Jacimovic et al.[8] turn out to be more flexible because of their mechanism basis. It can be seen that the models given by equation (4) with the new correlated constants gives quite good prediction for the clear liquid height for the small hole sieve tray. However, the suitability of the empirical correlation should be expected to be limited by the experimental conditions used to fit the constants.

4. Conclusions

Experimental results on the clear liquid height distribution along the flow path direction on small hole sieve trays for various operating conditions are reported. It is shown that the average clear liquid heights on small hole sieve tray increase with the increases of liquid flowrate and the height of outlet weir, but with decrease of the gas flowrate. Two semi-theoretical models developed by Bennett et al.[3] and Jacimovic et al.[8] respectively and a empirical correlation by Huang and Wang[9] are re-correlated and used to predict the clear liquid height for the small hole sieve tray. The model of Bennett et al.[3] and that of Jacimovic et al.[8], with the new correlated constants are shown to be more reliable for the prediction. The empirical correlation can also give adequate prediction but with lower flexibility.

References

1. P. A. M. Hofhuis and F. J. Zuiderweg, *IChemE Symposium Series*, 56(1979) 1–2.2.
2. C. J. Colwell, *Ind. Eng. Chem. Proc. Design and Development*, 20(1981) 298-307
3. D. L. Bennett,; R. Agrawal,; P. J. Cook, *AIChe J.* 29(1983) 434-442
4. H. Dhulesia, *IChemE Series* 62(1984 a) 321-326.
5. M. J. Lockett, *Distillation tray fundamentals*, Cambridge University Press, Cambridge: New York (1986)
6. E. Bekassy-Molnar and H. Mustafa, *IChemE Series* 69(1991a) 14-20
7. J. B. Francis, *Lowell Hydraulic Experiments*, 4th ed., Van Nostrand Company: New York, (1883)
8. B. M. Jacimovic and S. B. Genic, *Chem. Eng. Tech.* 23(2000) 171-176.
9. J. Huang and Z. C. Wang, *Chemical Engineering (in Chinese)*, 21(1993) 6-10

Appendix: Data of clear liquid heights on small hole sieve tray without outlet weir

L_W, m^3/(h.m)	F, (m/s).(kg/m^3)$^{0.5}$	x, cm								
		9	18	27	36	45	54	63	72	81
5	11.6	23.5	17.5	10.5	8	8.25	6.75	6.25	3	3.5
	15.4	20.5	13.5	10.5	9	6.75	6.25	5.25	3	3.5
	19.7	8.5	11.5	10.5	9	7.25	5.75	4.25	2	3.5
	24.1	8.5	12.5	10.5	8	5.25	5.75	3.25	1	1.5
	28.4	7.5	12.5	9.5	7	5.25	3.75	2.25	0	0
50	11.7	56.5	55.5	53.5	46	27.25	20.75	25.25	20	11.5
	15.4	57.5	55.5	46.5	22	22.25	22.75	19.25	14	9.5
	19.7	53.5	32.5	19.5	26	22.25	20.75	19.25	15	8.5
	24.1	42.5	18.5	13.5	25	23.25	18.75	14.25	10	5.5
	28.5	43.5	17.5	12.5	19	18.25	20.75	13.25	10	3.5
	33.1	44.5	17.5	9.5	12	14.25	18.75	14.25	10	2.5
	37.6	46.5	14.5	8.5	7	9.25	14.75	11.25	9	2.5